Supplementary Materials for

BDNF is a Negative Modulator of Morphine Action

Ja Wook Koo, Michelle S. Mazei-Robison, Dipesh Chaudhury, Barbara Juarez, Quincey LaPlant, Deveroux Ferguson, Jian Feng, Haosheng Sun, Kimberly Scobie, Diane Damez-Werno, Marshall Crumiller, Yoshinori N. Ohnishi, Yoko H. Ohnishi, Ezekiell Mouzon, David M. Dietz, Mary Kay Lobo, Rachael L. Neve, Scott J. Russo, Ming-Hu Han, and Eric J. Nestler

Correspondence to: Eric.Nestler@mssm.edu

This file includes:

Other Supplementary Material for this manuscript includes the following:

Tables S2 and S3

Supplemental Methods:

Animals and Drugs

Male 7~8-week-old c57BL/6 mice (25~30 g, Jackson), 9~13-week-old flBDNF, flTrkB (*3*), and DAT-cre/flTrkB mice (*17*) were fed *ad libitum*, and maintained at 22~25°C on a 12-hr light/dark cycle. All experiments were performed in accordance with guidelines of the Society for Neuroscience and the institutional animal care and use committee at Mount Sinai. The animals were acclimatized to vivarium conditions for at least one week before experimental manipulations. For microarrays and subsequent validations, flBDNF mice were lightly anesthetized with isofluorane and implanted subcutaneously with 2× 25 mg morphine pellets 48 hrs apart, then analyzed 48 hrs after the last pellet implantation. For *in vivo* recordings and whole cell recordings, c57BL/6 mice were implanted subcutaneously with one 25 mg morphine pellet, and analyzed 48 hrs later. Morphine pellets induce high, sustained levels of morphine in the blood and a strong degree of morphine dependence (*41*). For CPP, morphine sulfate was dissolved in sterile saline and administered (5~15 mg/kg, sc or ip). To measure levels of BDNF mRNA expression in VTA, morphine sulfate and/or cocaine-HCl in sterile saline was injected daily for 7 days (20 mg/kg, ip), with animals analyzed 24 hrs later.

Construction of Viral Vectors

For HSV-Sox11, we designed forward primer with *BamH*I restriction sites (5'-CGGGATCCCGATGGTGCAGCAGGCCGAGAGCTCGG-3') and reverse primer with *Xho*I restriction sites (5'-CCGCTCGAGCGGTCAATACGTGAACACCAGGTCGGAG-3'). For HSV-Gadd45g, we designed forward primer with *Kpn*I restriction sites (5'-GGGGTACCCC ATGACTCTGGAAGAAGTCCGTGGCC-3') and reverse primer with *Xho*I restriction sites (5'-CCGCTCGAGCGGTCACTCGGGAAGGGTGATGCTGGGC-3'). The coding sequences for *sox11* and *gadd45g* were subcloned into the bicistronic p1005+ HSV plasmid at *BamH*1-*Xho*I and *Kpn*I-*Xho*I, respectively. All behavioral experiments were began 2 or more days and finished by 5 days after viral

surgery and finished by 5 days post-surgery since HSV expression is maximal on days 2–4 post-infection (*42, 43*).

For AAV-shRNA-Sox11, two short hairpin RNAs (shRNA) were designed to target two specific regions of the *sox11* gene (GenBank accession NM_009234.6): GATACATAGGTCCTACTATGATAC and GATACAGCAACGTCATACAGTTTC. Each construct was ligated into pAAV-EGFP-shRNA as described previously (*44*). Positive clones were verified by PCR and sequencing. The vector plasmids were then packaged into AAV-2 particles using a helper-free plasmid transfection system in AAV-293 cells. The vector pAAV-eGFP was used for packaging the control viral vector AAV-GFP. Three days after transfection, cells were harvested, and the recombinant viral vector AAV-shRNA-Sox11 (or AAV-GFP) was purified using the AAV purification kit and concentrated using Amicon ultra according to the manufacturers' protocols. Viral titers were determined using quantitative PCR and ~1×10^9 particles/site were used for each viral injection.

Stereotaxic Surgery

Mice were anesthetized with a "cocktail" of ketamine (100 mg/kg/10 ml) and xylazine (10 mg/kg/10 ml) in sterile saline. 33 gauge needles were used to bilaterally infuse AAVs, HSVs, or BDNF (recombinant human BDNF) into VTA (AP = -3.2, ML = ±1.0, and DV = -4.6 from Bregma (mm); 7° angle) or NAc (AP = 1.5, ML = ±1.5, and DV = -4.4; 10° angle). An infusion volume of 0.5 µl was delivered using 5 µl Hamilton syringe over the course of 5 min (at a rate of 0.1 µl/min). The infusion needle remained in place for at least 5 min after the infusions before removal to prevent backflow of the injectate. For optic stimulation, a 20-guage guide cannula, 2 or 4 mm in length from the cannula base, was implanted unilaterally into the right hemisphere targeting NAc (AP = 1.5; ML = 1.3; DV = –3.9; 0° angle) or medial prefrontal cortex (mPFC) (AP = 1.7; ML = 0.4; DV = –1.7; 0° angle). BDNF (0.25 µg/side) was simultaneously bilaterally infused into the VTA, two weeks after bilateral AAV-EYFP-ChR2 or AAV-EYFP infusion into VTA. Mice were allowed to recover for seven days following the BDNF infusion

surgery and cannulation, and then used in CPP experiments. For *sox11* and *gadd45g* overexpression in NAc of VTA TrkB knockdown mice, we performed an intra-VTA infusion of AAV-CreGFP or AAV-GFP followed by intra-NAc infusion of HSV-Sox11 or HSV-Gadd45g two weeks later when the AAV virus was expressed and the mice cranium had healed from the first virus surgery. Mice were allowed to recover for two days following the HSV surgery, and then used in CPP experiments.

Morphine CPP

An unbiased CPP paradigm was used (*14*). Briefly, mice were placed in a three-chambered CPP box for 20 min to ensure no chamber bias. For the next three days, mice were conditioned to one chamber for 45 min in the morning (saline) and to the opposite chamber in the afternoon (0, 5, 10, 12.5, or 15 mg/kg morphine, sc or ip). A dose response of morphine CPP is shown in fig. S2. Sub-threshold (5~10 mg/kg) or moderate (12.5 mg/kg) doses of morphine were used to study reward potentiation, whereas higher doses (15 mg/kg) were used to study reward suppression. On day 5, CPP test day, mice were allowed to freely explore all three chambers for 20 min. For morphine/light CPP, optic fibers were secured to the cannula prior to saline or morphine (10 mg/kg, ip) injections. Mice were conditioned to saline/no light and morphine/blue light (473 nm, 20 Hz frequency, bursts of 5 light-pulses, 40 ms pulse duration, every 10 sec) for 30 min over two days and then tested as described above. CPP scores represent time spent in the paired – time spent in the unpaired chamber. Horizontal locomotor activity was measured during training sessions of morphine CPP.

RNA Isolation, Reverse Transcription, and RT-PCR

NAc or VTA punches (bilateral (NAc) or midline (VTA), 14-gauge) were freshly dissected on ice and held in ice-cold PBS solution from animals treated with indicated conditions and frozen on dry ice. Samples were homogenized in Trizol and processed with a micro RNeasy kit including a DNase I digestion according to the manufacturer's protocol. Spectroscopy confirmed RNA 260/280 and 260/230

ratios of >1.8. RNA was reverse transcribed into cDNA using an iScript cDNA synthesis kit. Primers were designed to amplify regions of 100-250 bp located within the gene (sequences shown below). SYBR Green quantitative PCR was carried out on a 7900HT with the following cycle parameters: 10 min at 95°C; 40 cycles of 95°C for 1 min, 60°C for 33 s, 72°C for 33 s; and graded heating to 95°C to generate dissociation curves for confirmation of single PCR products. All reactions were run in triplicate and analyzed using the ΔΔCt method as previously described (*45*) with glyceraldehyde-3-phosphate dehydrogenase (GAPDH) as a normalization control.

PCR primers

Target gene	Primer sequence (5' – 3')
gapdh	AACTTTGGCATTGTGGAAGG
gapdh_rev	ACACATTGGGGGTAGGAACA
bdnf-tot	CTCAGGCAGAATGAGCAATG
bdnf-tot_rev	AGCCGTCTGTGCTCTTCACT
trkB	TTG TGT GGC AGA AAA CCT TG
trkB _rev	ACA GTG AAT GGA ATG CAC CA
kcnab2	GGCCAGATCACGGATGAGATG
kcnab2_rev	AGCTTTTCCAGCAGCGTAGAC
kcnf1	CGTGGCAGGCGAAGACATT
kcnf1_rev	CCCCCGCCAAACAGTTGAT
kcnj2	ATGGGCAGTGTGAGAACCAAC
kcnj2_rev	TGGACTTTACTCTTGCCATTCC
kcnk4	AGAAGAAAATGGATCATGGCCG
kcnk4_rev	GGCTCTTCTGGCTCACACAGG
kcnq3	CCACCTTTTCTTTAATCGGCG
kcnq3_rev	CAGTGCCAGTCCTGAGCCAAG

girk1	CAGCAGCTGGTGCCCAAGAAG
girk1_rev	ACATGGGCTTTGTTCAGGTC
girk2	GTGAGGAAGGATGGGAAGTG
girk2_rev	AGACAAACCCGTTGAGGTTG
girk3	TCGTAGTCATTCTCGAGGGC
girk3_rev	CTGGGGATGGACCAGTAGAG
sox11	AGATGCGTTAGCTGCCTGAT
sox11_rev	CCCTTTGTACGCCATGCTAT
gadd45g	AGTCCTGAATGTGGACCCTG
gadd45g_rev	AGCAGAACGCCTGAATCAAC

Immunohistochemistry

Mice were anesthetized with a lethal dose of chloral hydrate and intracardially perfused with 0.1 M phosphate-buffered saline (PBS) and 4% (wt/vol) PBS-buffered paraformaldehyde. Post-fixed brains were incubated overnight in 30% sucrose at room temperature before being sliced on a microtome at 35 μm on a microtome. Free-floating sections were washed with PBS and then blocked in 3% bovine serum albumin (BSA) and 0.3% Triton-X for 1 hr. For GFP/Cre double-labeling in flBDNF mice, brain sections were incubated in 1:2000 of rabbit polyclonal anti-GFP (A11122, Invitrogen) and 1:1000 mouse anti-Cre recombinase (MAB3120) in block solution overnight at 4°C. The next day, sections were rinsed in PBS then incubated in 1:500 of donkey anti-rabbit Cy2 (Immuno Research) and 1:500 of donkey anti-mouse Cy3 in PBS for 1 hr then subsequently rinsed in PBS. To detect tdTomato (for HSV-Sox11 injection), 1:1000 of rabbit anti-dsRed (632496, Clontech) and then 1:500 of donkey anti-rabbit Cy3 were used. For EYFP (ChR2)/TH, EYFP (ChR2)/DAT, EYFP (ChR2)/GAD67, and EYFP (ChR2)/VGLUT2 double labeling, 1:4000 of anti-TH (T1299, Sigma), 1:5000 of anti-DAT (MAB369, Millipore), 1:1000 of anti-GAD67 (MAB5406, Millipore), or 1:2000 of anti-VGLUT2 (135 403, Synaptic systems) were used

respectively for overnight incubation with 1:1000 of rabbit anti-GFP (Invitrogen) or 1:1000 of chicken anti-GFP (GFP-1020, Aves) at 4°C. The next day, 1:500 of donkey anti-Rat Cy3 (Immuno Research) for anti-DAT, 1:500 of donkey anti-mouse Cy3 for anti-GAD67, and 1:500 of donkey anti-rabbit Cy3 for anti-VGLUT2 were respectively used in PBS together with 1:500 of donkey anti-rabbit Cy2 or donkey anti-chicken Cy2. All sections were counterstained and mounted with antifade solution, including DAPI then subsequently imaged on a LSM 710 confocal microscope.

In Vivo Recordings

In vivo extracellular, single-unit recordings from the VTA DA neurons of anesthetized intact mice were conducted following published methods (*46-48*). Control, morphine-pelleted (25 mg) and/or VTA BDNF-infused c57/BL6 mice were anesthetized with 8% chloral hydrate (400 mg/kg, ip). Intra-VTA AAV-GFP or AAV-CreGFP infused flBDNF mice also were used for recordings. VTA coordinates were measured from the bregma and were as follows (in mm): AP = -2.92~-3.88; ML = ±0.24~0.96; and DV = -3.5~-4.5. Using a DP-311 Differential Amplifier, extracellular single-unit signals were amplified and filtered (0.3-1 kHz band-pass). Voltage data were acquired using an Axon Digidata Data Acquisition System, sampled using 16-bit resolution at 32 kHz, and stored using pCLAMP for further offline analysis. Putative DA cells in the VTA were identified according to standard electrophysiological criteria: a stark, triphasic waveform; action potential duration from start to negative trough >1.1 ms; slow firing rate (<10 spikes/s); and slow, bursting behavior. Data were digitally band-pass filtered (300-7000 Hz) using MATLAB offline analysis software. Voltage traces were thresholded by eye, and spike waveforms extracted and up-sampled to 128 kHz using spline interpolation to better estimate spike peak time. Principal Component Analysis was used to extract spike waveform coefficients, and clustering was performed using k-means sorting. Bursts were defined as a series of spikes initiated by an inter-spike interval (ISI) of <80ms and terminated by an ISI of >160ms. The extent of bursting in each neuron was quantified by the percentage of total spikes located in a burst sequence, the proportion of total time spent

in a bursting state, and finally by the frequency of burst onset.

Whole-Cell Recordings

Whole–cell voltage-clamp recordings were obtained from VTA DA neurons in acute brain slices from c57BL/6 mice that had been previously treated with PBS, PBS+morphine or BDNF+morphine. All recordings were carried out blind to the experimental conditions of the mice. To minimize stress and to obtain healthy VTA slices, mice were anesthetized prior to decapitation and the brain was rapidly removed and placed in ice cold sucrose-aCSF (artificial cerebrospinal fluid), which contained: 254 mM sucrose, 3 mM KCl, 1.25 mM NaH_2PO4, 10 mM D-glucose, 24 mM $NaHCO_3$, 2 mM $CaCl_2$ and 2 mM $MgCl_2$ (oxygenated with 95% O_2 and 5% CO_2, pH 7.4, 295~305 mOsm), for 1 min. Acute brain slices containing the VTA were cut using a microslicer in cold sucrose-aCSF. Slices were maintained for 1 hour at 37^{o}C in a holding chamber with regular aCSF, which contained: 128 mM NaCl, 3 mM KCl, 1.25 mM NaH_2PO4, 10 mM D-glucose, 25 mM $NaHCO_3$, 2 mM $CaCl_2$ and 2 mM $MgCl_2$ (saturated with 95% O_2 and 5% CO_2, pH 7.4, 295~305 mOsm). Patch pipettes (3-5 mΩ) for voltage-clamp recordings were filled with internal solution: 115 mM potassium gluconate, 20 mM KCl, 1.5 mM $MgCl_2$, 10 mM phosphocreatine, 10 mM HEPES, 2 mM magnesium ATP and 0.5 mM GTP (pH 7.2, 285 mOsm). Whole-cell recordings were carried out in aCSF at 34^{o}C (flow rate = 2.5 ml/min). To isolate potassium (K^+) currents during whole-cell recordings, tetrodotoxin (TTX; 1 μM), cadmium chloride ($CdCl_2$; 200 μM), kynurenic acid (1 mM) and picrotoxin (100 μM) were added to bath aCSF solution in order to block sodium channels, calcium channels, glutamate receptors and $GABA_A$ receptors, respectively. In all recordings, cells were held at -70 mV. Putative VTA DA neurons were electrophysiologically identified by the presence of hyperpolarization-activated current (I_h) during 10 mV incremental voltage steps ranging from -60 to 0 mV (*49*). K^+ currents of VTA DA cells, in response to depolarizing voltage steps ranging from 0 to +90 mV (in increments of 10 mV) was measured using the Multiclamp 700B amplifier and data acquisition was done in pClamp 10. Series resistance was monitored during the experiments and

membrane currents were filtered at 3 kHz (Bessel filter).

In Vivo Optogenetic Stimulation

For *in vivo* optical stimulation one week after cannulation and BDNF infusion, a 200 μm core optic fiber was modified for attachment to the cannula. Optic fibers were attached through an FC/PC adaptor to a 473 nm blue laser diode, and light pulses were generated through a stimulator. When the optic fiber was placed to the head-mount cannula, the fiber was flush with ~50 μm of the stripped 200 μm core exposed beyond the cannula as described in previous study (*7, 24*). Bursts of 5 light-pulses (40 ms pulse duration, 15.9-27.8 mW/mm^2 irradiance) at a frequency of 10, 20, 30, or 50 Hz were delivered into NAc every 10 sec, which were used to determine spike fidelity similar to what was obtained during *in vivo* recording. Spike fidelity was maintained for frequencies up to 20 Hz, but was lower than the stimulating frequencies at 30 or 50 Hz (not shown), as reported by others (*24*). For NAc microinjection of receptor antagonists, a 33-gauge injector needle that was engineered with 24 gauge-steel tubing was connected to a 10 μl Hamilton syringe by vinyl tubing (V/3). Unilateral microinjections of SCH 23390 (D1 receptor antagonist, 1 μg/0.5 μl/side) (*25, 26*), eticlopride (D2 receptor antagonist, 1 or 4 μg/0.5 μl/side) (*29*), DNQX (6,7-dinitroquinoxaline-2,3-dione, AMPA receptor antagonist, 1 or 4 μg/0.5 μl/side) (*27*), NBQX (2,3-dihydroxy-6-nitro-7-sulfamoyl-benzo[f]quinoxaline-2,3-dione, another AMPA receptor antagonist, 0.4 μg/0.5 μl/side) (*28*), or sterile saline (vehicle) were delivered through an injector needle at a continuous rate of 0.1 μl/min under the control of a micro-infusion pump. Injector needles remained in place for 4~5 min before being pulled out and replaced immediately with optical fibers for morphine CPP training to prevent backflow of the injectate through the guide cannula.

Microarrays

NAc tissues (bilateral, 14 gauge) were obtained from intact or morphine-pelleted (25 mg ×2) mice in control or VTA BDNF knockdown conditions. Three biological replicates were performed for

each group, each consisting of mRNA pooled from three mice. RNA was isolated with Trizol, further purified with the RNAeasy micro kit, and checked for quality with Bioanalyzer, prior to labeling and hybridization onto the mouse gene 1.0 st array. Raw data were background subtracted, quantile normalized, and then analyzed with Genespring GX 10.0. Two-way ANOVA was used for analysis, followed by Tukey's post-hoc tests. The p-values were calculated using Welch's test and corrected by Benjamini-Hochberg False Discovery Rate method. Genelists were generated with significance criteria of 1.3 fold change cutoff coupled with a non-stringent cutoff of $p < 0.05$.

Statistics

Student's t-tests were used for the analysis of studies with two experimental groups. One-way ANOVA was used for analysis of three or more groups, followed by Fisher's PLSD post-hoc tests, when appropriate. Microarray data was analyzed using two-way ANOVA, followed by Fisher's PLSD post-hoc tests. For the whole cell recording data and the locomotor activity data, a repeated-measure two-way ANOVA was used followed by Fisher's PLSD post-hoc tests, if appropriate. Main and interaction effects were considered significant at $p < 0.05$. All data are expressed as mean ± SEM.

Fig. S1

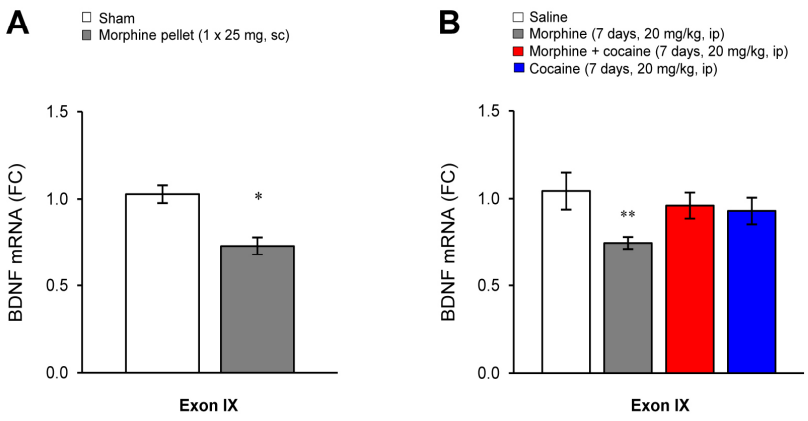

Fig. S1. Regulation of BDNF expression in VTA by morphine and cocaine.

(A) Morphine given by pellet implantation (25 mg, sc) decreases the mRNA expression of *bdnf* (exon 9) in VTA. Student's t-test, $*p < 0.05$, n = 8-9. (B) Repeated morphine injections (7 days, 20 mg/kg, ip, animals analyzed 24 hrs after last injection) also reduced VTA *bdnf* mRNA expression. However, repeated cocaine injections (7 days, 20 mg/kg, ip), which by themselves had no effect on VTA *bdnf* expression, blocked the ability of concomitant morphine to suppress *bdnf* mRNA levels. One-way ANOVA, Fisher's PLSD test, $**p < 0.01$, compared with control. n = 9-10.

Fig. S2

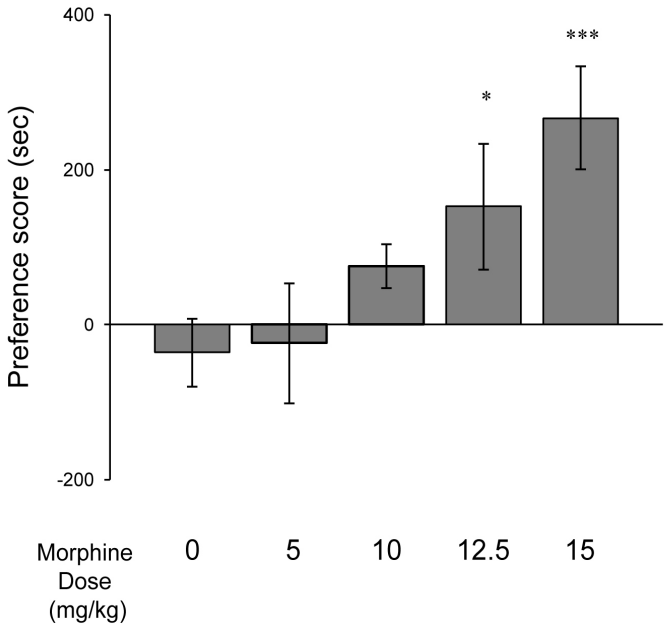

Fig. S2. Dose-response analysis of morphine CPP.

Morphine was injected at varying doses (5~15 mg/kg) during CPP training. One-way ANOVA, Fisher's PLSD test, *$p < 0.05$, ***$p < 0.001$, compared with saline-injected controls (0 mg/kg), n = 10-20.

Fig. S3

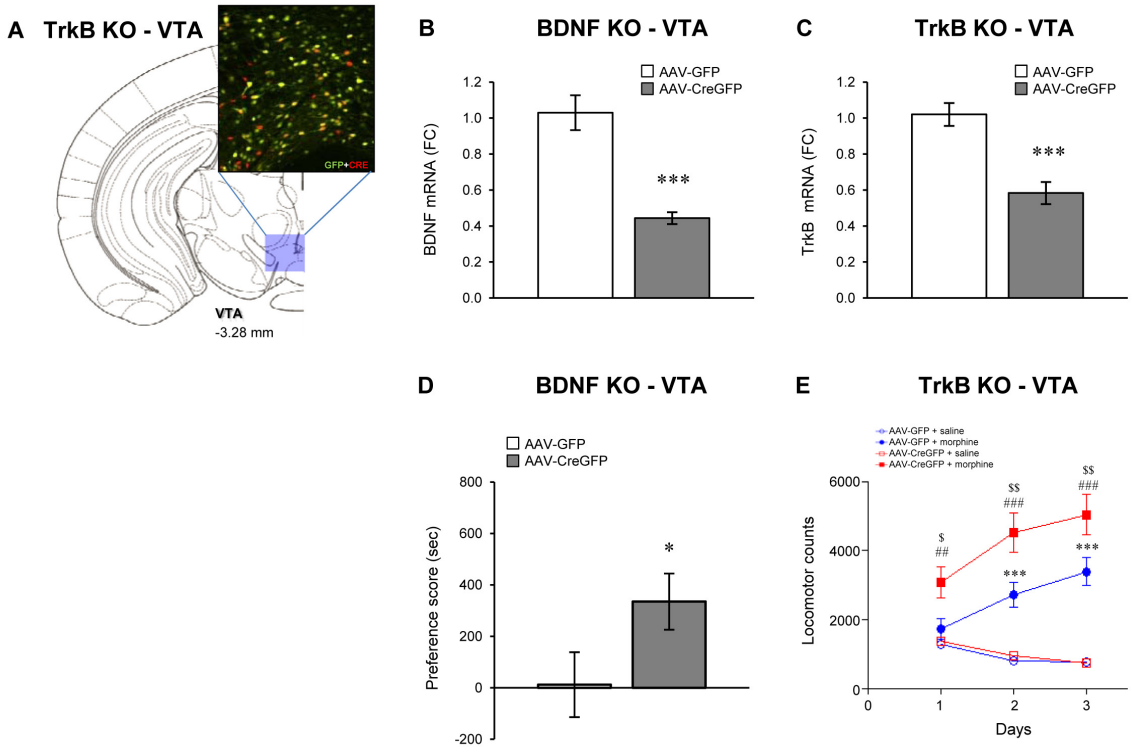

Fig. S3. Local knockdown of BDNF and TrkB in VTA and its effects on morphine CPP and locomotor activity.

(A) Schematic coronal sections from VTA with an inset depicting localized AAV-mediated GFP (green)/Cre (red) expression in VTA neurons. (B to C) Validation of AAV-CreGFP-mediated gene ablation in VTA of flBDNF and of flTrkB mice. RT-PCR with VTA tissues infected with AAV-CreGFP show a 55.6% reduction in BDNF mRNA in VTA of flBDNF mice (B, Student's t-test, ***$p < 0.001$, n = 7-8) and a 41.7% reduction in TrkB mRNA in VTA of flTrkB mice (C, ***$p < 0.001$, n = 11-14), compared with AAV-GFP-infected controls, findings consistent with previous studies (*3, 8, 50, 51*). (D) Localized BDNF KO in VTA increases CPP with a sub-threshold 5 mg/kg dose of morphine, as seen for a high (15 mg/kg) as well (Fig. 1A). *$p < 0.05$, n = 8-10. (E) Localized TrkB KO in VTA increases locomotor activity during the morphine pairing sessions (repeated measures two-way ANOVA, treatment effect: $p<0.001$; treatment×day effect: $p<0.001$). ***$p<0.001$ compared with AAV-GFP-saline group; $^{\#\#}p<0.01$, $^{\#\#\#}p<0.001$ compared with AAV-CreGFP-saline group; $^{\$}p<0.05$, $^{\$\$}p<0.01$ compared with AAV-GFP-morphine group in Fisher's PLSD test, n = 9-11.

Fig. S4

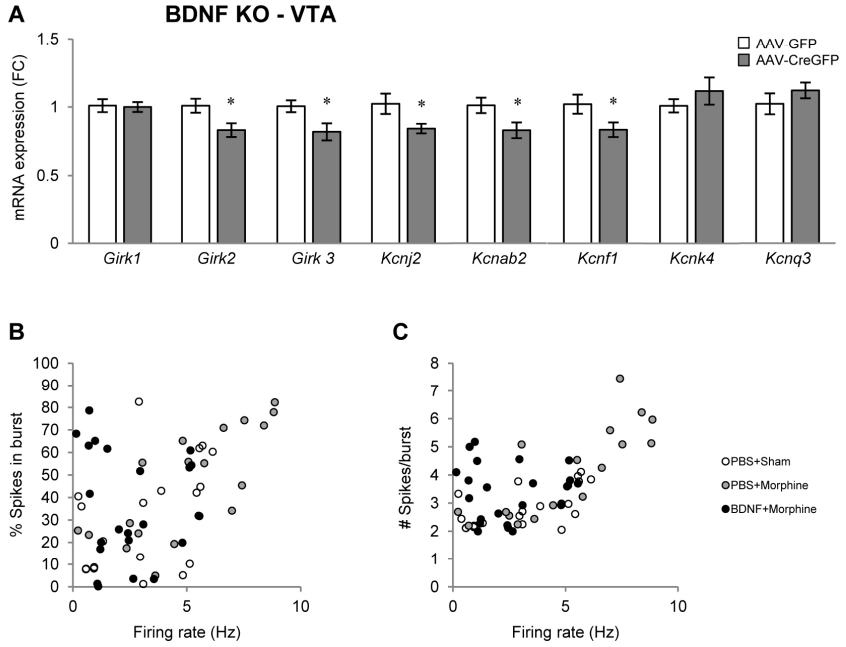

Fig. S4. Regulation of VTA K^+ channel subunit expression and VTA DA excitability by BDNF.
(A) VTA BDNF knockdown decreases the mRNA expression of certain K^+ channel subunits such as *girk2, girk3*, *kcnj2, kcnab2,* and *kcnf1,* but not *girk1*, *kcnk4,* and *kcnq3* in VTA. Student's t-test, *$p < 0.05$, n = 9-10. (B and C) Scatter plot of the bursting activity and firing rates of all neurons recorded from PBS control, morphine-treated, and BDNF+morphine-treated mice. (B) Firing rates are significantly positively correlated with percentage of spikes in bursts in PBS control, morphine-treated groups (control: $r^2 = 0.197$, n = 19 cells/4 mice, $p < 0.05$; morphine-treated: $r^2 = 0.554$, n = 19 cells/4 mice, $p < 0.001$), but not in BDNF+morphine-treated mice ($r^2 = 0.0758$, n = 23 cells/6 mice, p = ns). (C) Firing rates are also significantly positively correlated with percentage of burst size (i.e., number of spikes per burst) in PBS control, morphine-treated groups (control: $r^2 = 0.369$, $p < 0.01$; morphine-treated: $r^2 = 0.631$, $p < 0.001$), but not in BDNF+morphine-treated mice ($r^2 < 0.0001$, p = ns).

Fig. S5

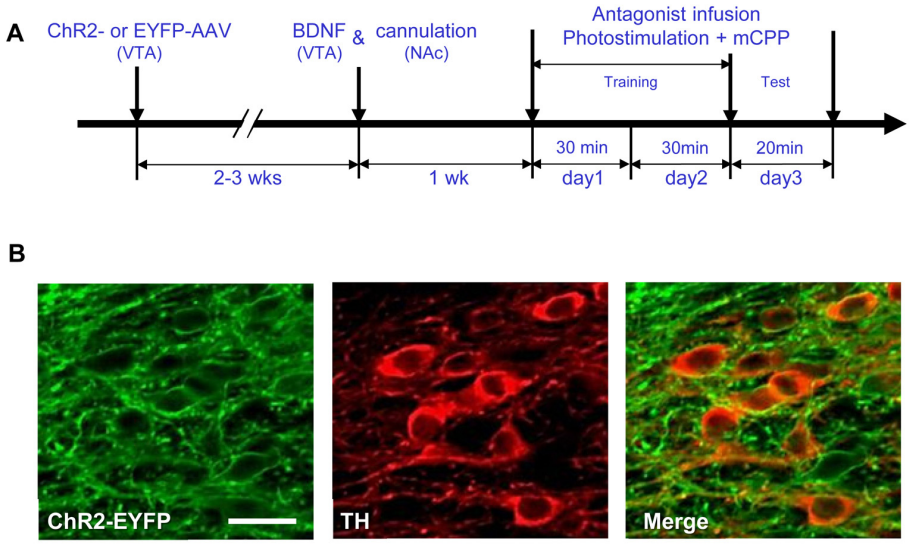

Fig. S5. Experimental paradigm used for *in vivo* optogenetic stimulation during morphine CPP.
(A) A schematic diagram depicting the experimental procedures for optical stimulation and D1, D2, or AMPA receptor antagonism in morphine CPP. 2-3 weeks after delivery of AAV-ChR2 (channel rhodopsin)-EYFP or AAV-EYFP into VTA and 1 week prior to the morphine CPP experiment, we infused BDNF into VTA and implanted cannulae in NAc for optic fiber placement. 10 min before the optical stimulation during 30 min morphine CPP training session, either appropriate antagonists or vehicle (saline) was delivered into the unilateral stimulating site in NAc. After 2 day training, the animals were tested for 20 min to check place preference. (B) Immunostaining for ChR2-EYFP (left, green) and TH (middle, red) in VTA. Confocal microscopy shows that 86.0% of ChR2-EYFP positive cells co-labeled with TH (right). Scale bar, 20 μm.

Fig. S6

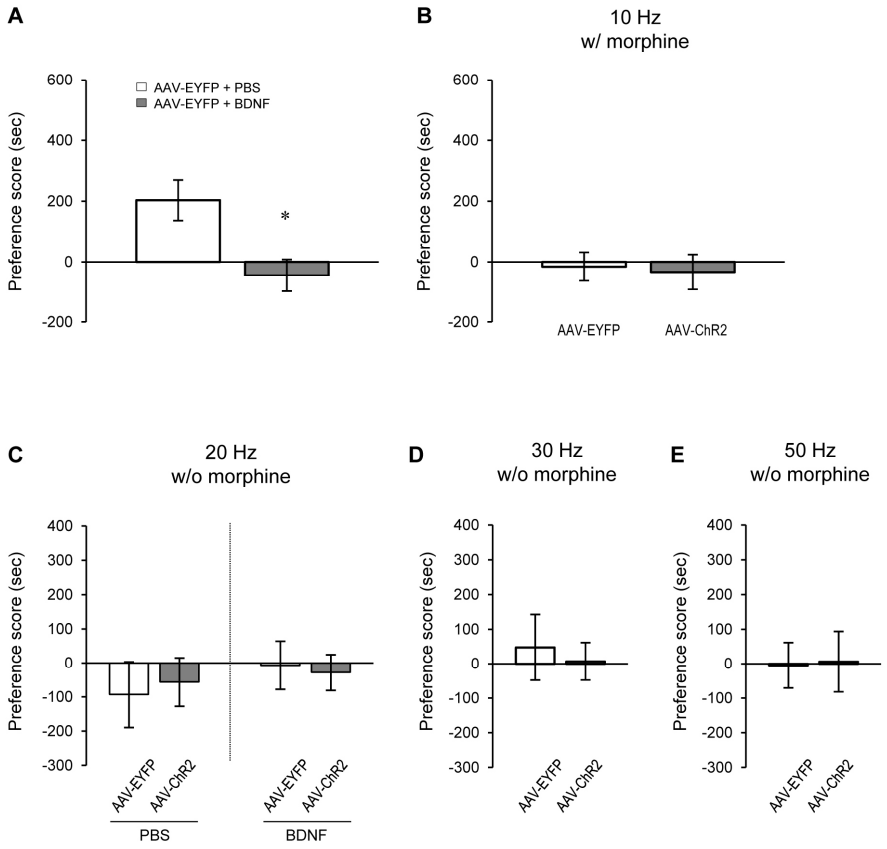

Fig. S6. Effects of *in vivo* optogenetic stimulation at various frequencies on CPP.

(A) The ability of intra-VTA BDNF (0.25 μg/side) to attenuate morphine CPP, as observed in mice with no other manipulations (see Fig. 1D), is also observed in mice with prior intra-VTA infusion of AAV-EYFP. This indicates that there is no interaction per se between intra-VTA injections of BDNF and AAV-EYFP with respect to morphine reward. Student's t-test, $*p < 0.05$, n = 8. (B) Optical stimulation with 10 Hz frequency did not induce morphine CPP, which is in contrast to the ability of 20 Hz stimulation to have this effect (see Fig. 3K). (C to E) Optical stimulation by itself (i.e., without morphine) at 20 Hz (C), 30 Hz (D), or 50 Hz (E) in naïve or VTA BDNF-infused mice did not induce a CPP. There was no difference in baseline scores. Prior work has shown that 50 Hz stimulation of VTA DA neuron cell bodies is capable of inducing a CPP in the absence of a drug of abuse (*24*). The failure of 50 Hz stimulation of DA nerve terminals in NAc to induce a CPP likely reflects the requirement of projections of VTA DA neurons to brain regions in addition to the NAc in mediating this effect.

Fig. S7

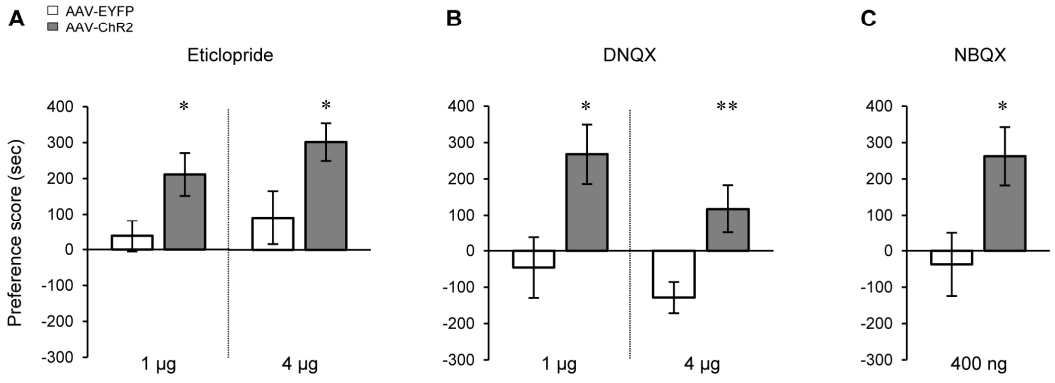

Fig. S7. Effect of *in vivo* optogenetic stimulation with D2 and AMPA antagonism on morphine CPP. (A) Intra-NAc injection of a D2 receptor antagonist (eticlopride, 1 or 4 µg) or an AMPA receptor antagonist (DNQX, 1or 4 µg; or NBQX, 400 ng) did not affect the ability of optical stimulation (20 Hz) of DA terminals in the NAc to promote morphine CPP (10 mg/kg). Each of these doses has been shown to be behaviorally active in other paradigms (*25-29*). There was no difference in baseline scores. Student's t-test, $*p < 0.05$, $**p < 0.01$, n = 9-10.

Fig. S8

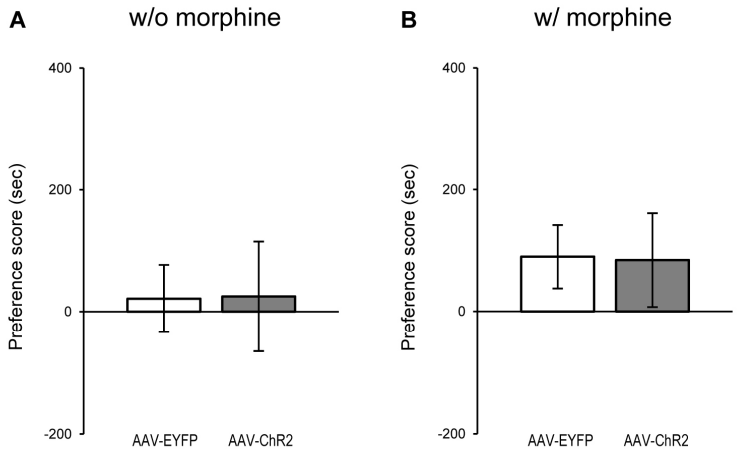

Fig. S8. Lack of modulation of morphine reward by optogenetic activation of DA terminals in mPFC.

(A and B) Optical stimulation (20 Hz) of the mPFC, 3-4 weeks after intra-VTA injections of AAV-ChR2-EYFP or AAV-EYFP, had no effect on CPP in the absence or presence of morphine (10 mg/kg).

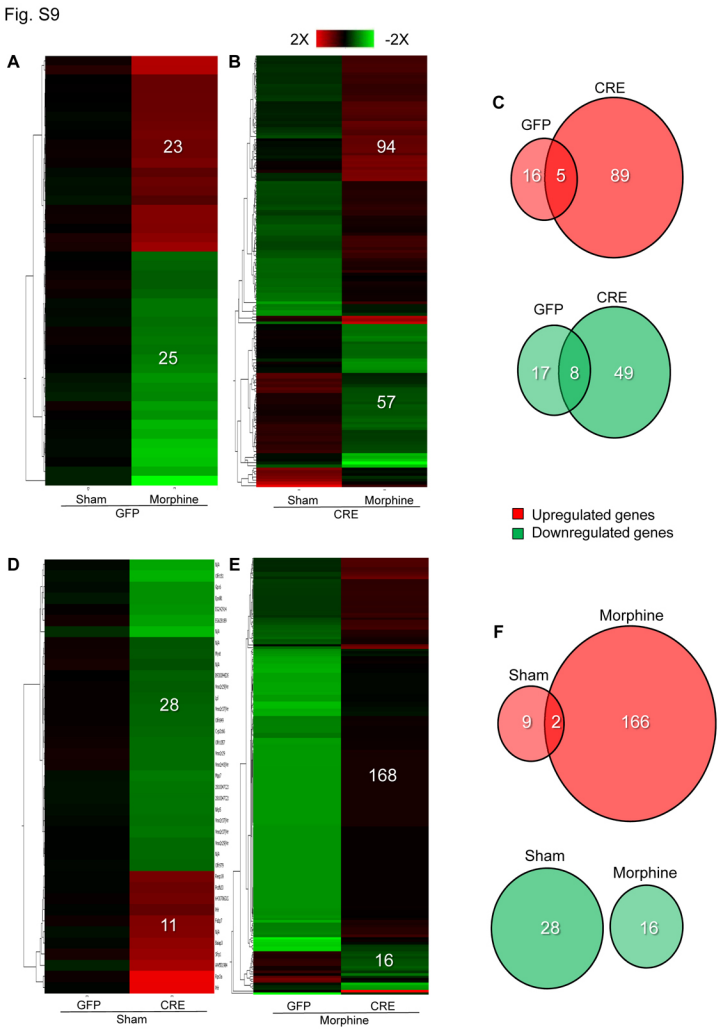

Fig. S9. Microarray analysis of morphine-regulated NAc gene expression after VTA BDNF Deletion. Student's t-tests were used to compare the different treatment conditions. (A) Heatmap of up- or down-regulated NAc genes by morphine in naïve mice (criteria for significance: ≥1.3-fold change compared to sham/GFP group at $p < 0.05$ in t-test). (B) Heatmap of up- or down-regulated NAc genes by morphine in VTA BDNF knockdown mice (compared to sham/Cre group at $p < 0.05$) (C) Venn diagrams of up- (red) or down- (green) regulated NAc genes by morphine in naïve and VTA BDNF knockdown animals. (D) Heatmap of up- or down-regulated NAc genes by VTA BDNF knockdown in sham mice (compared to sham/GFP group at $p < 0.05$). (E) Heatmap of up- or down-regulated NAc genes by VTA BDNF knockdown in morphine-pelleted mice (compared to morphine/GFP group at $p < 0.05$). (F) Venn diagrams of up-(red) or down-(green) regulated NAc genes by VTA BDNF knockdown in sham and morphine-treated mice.

Fig. S10

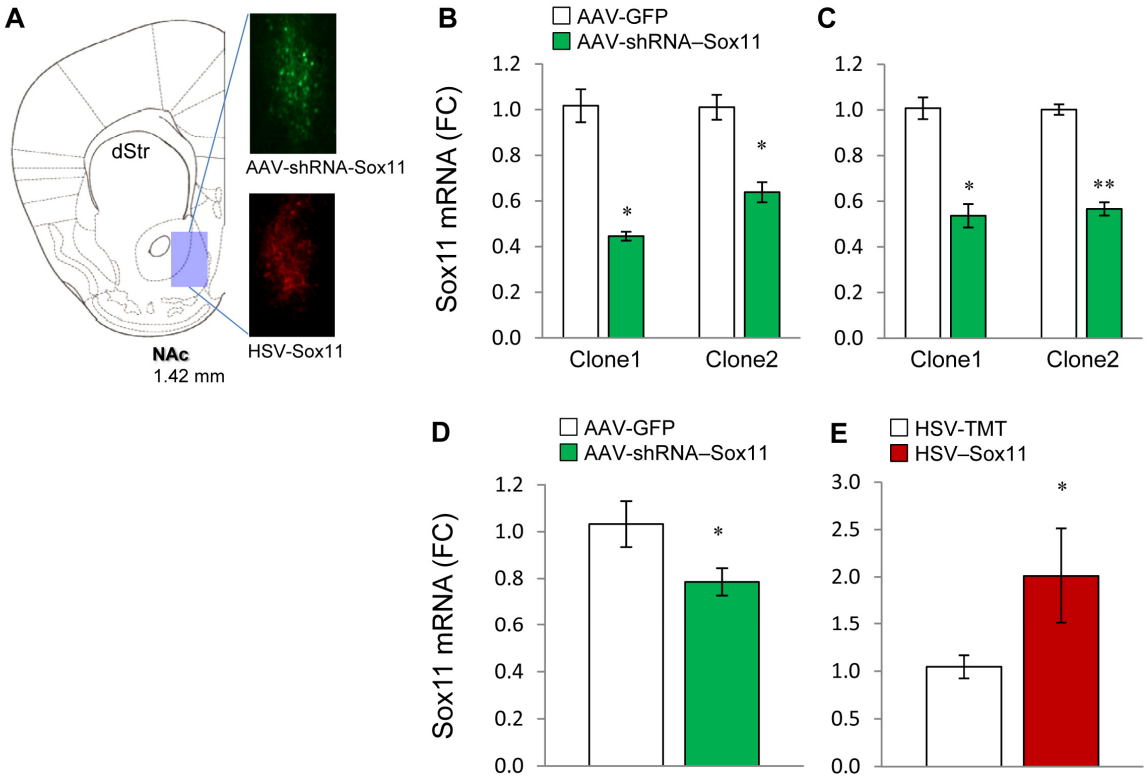

Fig. S10. Validation of AAV-shRNA-Sox11 and HSV-Sox11 in Neuro2A cells and in NAc.

(A) Representative photograph of injection of AAV-shRNA-Sox11 (GFP+, green) or HSV-Sox11 (tdTomato (TMT)+, red) in NAc. (B and C) Transfection of Neuro2A cells with AAV-shRNA-Sox11 for 24 (B, clone1: $*p < 0.05$, n = 3; clone2: $*p < 0.05$, n = 3) or 48 hrs (C, clone1: $*p < 0.05$, n = 3; clone2: $**p < 0.01$. n = 3) reduces levels of *sox11* mRNA expression. (D) Infusion of AAV-shRNA-Sox11 into NAc decreases *sox11* mRNA expression ($*p < 0.05$, n = 9). (E) In contrast, intra-NAc infusion of HSV-Sox11 increases *sox11* mRNA expression ($*p < 0.05$, n = 8).

Fig. S11

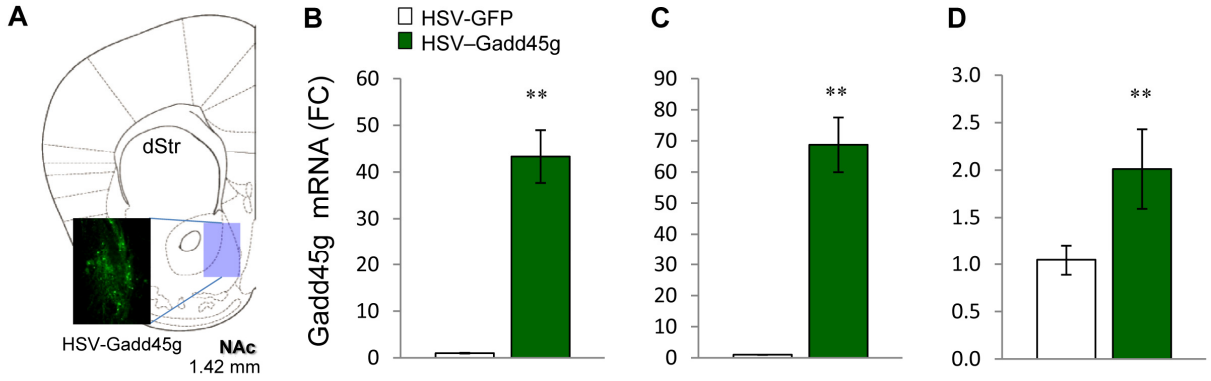

Fig. S11. Validation of HSV-Gadd45g in Neuro2A cells and in NAc.

(A) Representative photograph of injection of HSV-Gadd45g in NAc. Infected cells express GFP (green). (B and C) Incubation with HSV-Gadd45g in Neuro2A cells for 24 (B, Student's t-test, $^{**}p < 0.01$, n = 3) or 48 hrs (C, $^{**}p < 0.01$, n = 3) showed robust augmentation of *gadd45g* mRNA expression. (D) Infusion of HSV-Gadd45g into NAc increased levels of *gadd45g* mRNA expression (χ^2 test, $^{**}p < 0.01$, n = 7).

Fig. S12

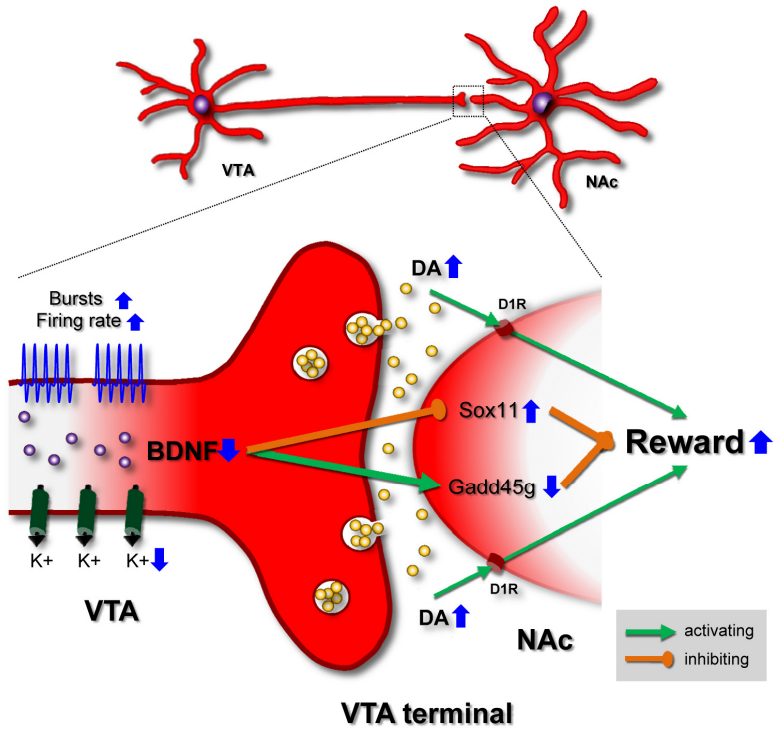

Fig. S12. Model for BDNF-morphine interactions in the VTA-NAc.

Suppression of BDNF expression in VTA by chronic morphine reduces the expression of certain K^+ channel subunits and K^+ conductance in these neurons and concomitantly enhances VTA DA cell firing and burst activity. The burst-like phasic firing induces high levels of DA release in NAc (*19, 20*), which primarily activates D1 receptors (*19, 30*). Reduced VTA BDNF influences chronic morphine regulation of gene expression in NAc, e.g., *sox11* and *gadd45g*. The net effect of these actions of suppressed VTA BDNF is to promote morphine reward as measured by CPP. DA transmission promotes morphine reward in part by increasing the incentive salience of morphine-paired cues (*52*). Morphine reward is also mediated by DA-independent mechanisms. Moreover, compulsive morphine use is driven in part by negative reinforcement—that is, to alleviate withdrawal (*53*). Further work is needed to study the influence of BDNF signaling in VTA on these various components of morphine action. In addition, exogenous BDNF has been reported to promote a shift from DA-independent to DA-dependent reward via a switch in $GABA_A$ receptor signaling, from inhibitory to excitatory, on rat VTA GABAergic neurons (*10*). Reduced BDNF expression in VTA might contribute to the induction of VTA DA excitability by interfering with this switch in VTA GABA signaling. These observations suggest that neural substrates (GABA vs. DA) of BDNF within the VTA might differ according to species, morphine treatment paradigms, and CPP protocols utilized.

Table S1. Summary table of NAc genes significantly up- or down-regulated by morphine or by VTA BDNF KO. *p<0.05, morphine or BDNF knockdown effect. SRY, Sex-determining region Y; BTB, bric-a-brac tramtrack broad complex; GDNF, glial cell line-derived neurotrophic factor.

Table S1

• Gene regulation by morphine lost upon knockdown of BDNF in VTA			
UP	*Sox11* (SRY-box containing gene 11) *Mc4r* (Melanocortin 4 receptor) *Zfp40** (Zinc finger protein 4) *Krt9* (Keratin 9) *Dhrs3* (Dehydrogenase/reductase member 3) *Tubd1** (Tubulin, delta 1) *Tra2a** (Transformer 2 alpha homolog)	Down	*Gpx6* (Glutathione peroxidase 6) *Arsg* (Arylsulfatase G) *Cnp* (2',3'-cyclic nucleotide 3' phosphodiesterase) *Mog* (Myelin oligodendrocyte glycoprotein) *Aspa* (Aspartoacylase) *Tmem16b** (Transmembrane protein 16B) *Sept4* (Septin 4)
• Gene regulation by morphine uncovered upon knockdown of BDNF in VTA			
UP	*Xdh** (Xanthine dehydrogenase) *Zbtb16* (Zinc finger and BTB domain containing 16) *Htr2a** (5-hydroxytryptamine (serotonin) receptor 2A) *Slc4a11** (Solute carrier family4, sodium bicarbonate transporter-like, member 11) *Gfral* (GDNF family receptor alpha like) *Cyp2c66** (Cytochrome P450, family 2, subfamily c, polypeptide 66) *Bglap-rs1** (Bone gamma-carboxyglutamate protein, related sequence 1) *Hif3a* (Hypoxia inducible factor 3, alpha subunit) *Fscn3** (Fascin homolog 3, actin-bundling protein, testicular)	Down	*Fut11** (Fucosyltransferase 11) *Gadd45g** (Growth arrest and DNA-damage-inducible 45 gamma) *Nr4a1** (Nuclear receptor subfamily 4, group A, member 1) *Fabp7** (Fatty acid binding protein 7, brain) *Insig1** (Insulin induced gene 1) *Idi1* (Isopentenyl-diphosphate delta isomerase) *Hmcn1** (Hemicentin 1) *Sqle* (Squalene epoxidase) *Scd1* (Stearoyl-Coenzyme A desaturase 1) *Rreb1* (Ras responsive element binding protein 1)
• Gene regulation by morphine regardless of VTA BDNF knockdown			
UP	*Nt5e* (5' nucleotidase, ecto) *Sult1a1* (Sulfotransferase family 1A, phenol-preferring, member 1) *Bcl2*|LOC100046608 (B-cell leukemia/lymphoma 2) *Hrh3* (Histamine receptor H3)	Down	*Rbm3* (RNA binding motif protein 3) *Cirbp* (Cold inducible RNA binding protein) *Serpinb1a* (Serine peptidase inhibitor, clade B, member 1a) *Hmgcs1*|LOC100040592 (3-hydroxy-3-methylglutaryl-Coenzyme A synthase 1) *Slc16a1* (Solute carrier family 16, member 1)

Table S2. Microarray gene list based on two-way ANOVA (provided as separate Excel file).

Table S3. Microarray gene list based on student's t-test (provided as separate Excel file).

Supplemental References:

41. S. J. Fischer *et al.*, *Neuroscience* **151**, 1217 (2008).
42. M. Barrot *et al.*, *Proc Natl Acad Sci U S A* **99**, 11435 (2002).
43. W. A. Carlezon, Jr. *et al.*, *Science* **282**, 2272 (1998).
44. J. D. Hommel, R. M. Sears, D. Georgescu, D. L. Simmons, R. J. DiLeone, *Nat Med* **9**, 1539 (2003).
45. K. J. Livak, T. D. Schmittgen, *Methods* **25**, 402 (2001).
46. J. L. Cao *et al.*, *J Neurosci* **30**, 16453 (2010).
47. M. Mameli-Engvall *et al.*, *Neuron* **50**, 911 (2006).
48. C. A. McClung *et al.*, *Proc Natl Acad Sci U S A* **102**, 9377 (2005).
49. D. Saal, Y. Dong, A. Bonci, R. C. Malenka, *Neuron* **37**, 577 (2003).
50. V. Krishnan *et al.*, *Cell* **131**, 391 (2007).
51. O. Berton *et al.*, *Science* **311**, 864 (2006).
52. K. C. Berridge, *Psychopharmacology (Berl)* **191**, 391 (2007).
53. G. F. Koob, M. Le Moal, *Philos Trans R Soc Lond B Biol Sci* **363**, 3113 (2008).